Effects of Vitiation and Pressure on Laminar Flame Speeds of *n*-Decane

C. C. Fuller[1], P. Gokulakrishnan[2], and M. S. Klassen[3]
Combustion Science & Engineering, Inc., Columbia, MD 21045

S. Adusumilli[4], Y. Kochar[4], D. Bloomer[4] and J. Seitzman[5]
School of Aerospace Engineering, Georgia Institute of Technology, Atlanta, GA, 30332

H. H. Kim[6], S. H. Won[7], F. L. Dryer[8] and Y. Ju[9]
Department of Mechanical and Aerospace Engineering, Princeton University, Princeton, NJ, 08544

B. V. Kiel[10]
Air Force Research Laboratory, Wright Patterson Air Force Base, Dayton, OH, 45433

There is currently a lack of experimental data required for kinetic model validation of the effect of oxidizer vitiation on laminar flame speeds of aviation fuels. This study examines the role of vitiation through the introduction of CO_2 and H_2O to the oxidizer stream at varying pressures (0.5 - 5.0 atm) at 450 K, conditions relevant to vitiated combustion devices, using *n*-decane as the model fuel. The experimental portion of this effort has acquired laminar flame speed data of *n*-decane in vitiated air using two separate techniques. A well-validated Bunsen Flame Technique was used to primarily examine the effect of total dilution and vitiation over a range of equivalence ratios and the Combustion Bomb Technique was used to investigate vitiation effects at various pressures and equivalence ratios. Overlap between measurement techniques has been performed as well as comparison to an analytical model to better understand the thermodynamic and chemical kinetic effects that vitiation has on hydrocarbon fuel combustion and flame structure. Experimental data shows that CO_2 has the largest effect in reducing the flame speed over the range of equivalence ratios and pressures studied. Based on a kinetic analysis, chemical kinetic effects play a major role in reducing the flame speed when CO_2 is present. The impact of chemical kinetic effects due to the diluent species on flame speed was found to have the following trend: $CO_2 > H_2O > N_2$.

Nomenclature

X_n	=	mole fraction concentration of species n given [mole or vol %]
Φ	=	fuel:air equivalence ratio: $(fuel/air)/(fuel/air)_{stoich}$
T_{Ad}	=	adiabatic flame temperature [K]
C_P	=	molar heat capacity [J/mol-K]
α	=	thermal diffusivity [m^2/s]
BFT	=	Bunsen Flame Technique
CBT	=	Combustion Bomb Technique

---

[1] Project Engineer, Combustion Science and Engineering, Inc., Member AIAA
[2] Principal Engineer, Combustion Science and Engineering, Inc., Senior Member AIAA
[3] Principal Research Engineer, Combustion Science and Engineering, Inc., Senior Member AIAA
[4] Graduate Student, School of Aerospace Engineering, Georgia Institute of Technology
[5] Professor, School of Aerospace Engineering, Georgia Institute of Technology, Associate Fellow AIAA
[6] Graduate Student, Dept. of Mechanical and Aerospace Engineering, Princeton University
[7] Assoc. Research Scholar, Dept. of Mechanical and Aerospace Engineering, Princeton University, Member AIAA
[8] Professor, Dept. of Mechanical and Aerospace Engineering, Princeton University, Associate Fellow AIAA
[9] Assoc. Professor, Dept. of Mechanical and Aerospace Engineering, Princeton University, Associate Fellow AIAA
[10] Augmentor Technology Lead, RZTC, 1950 5th Street, WPAFB, Senior Member AIAA

Introduction

Vitiated air is commonly encountered in combustion applications in which exhaust gas is recycled back into the oxidizer stream in order to increase the combustion efficiency and to reduce pollutant emissions. In essence, the addition of combustion product gases into the incoming air impacts the oxidation kinetics of the fuel and the flame propagation due to the change in the O_2 concentration as well as the presence of CO_2, H_2O, CO, NO_X, and unburned hydrocarbons in the oxidizer stream. Accurate chemical kinetic model predictions of the fuel oxidation in the presence of vitiated air become a challenging task, especially for hydrocarbon fuels, due to the complex chemical kinetic interaction of the vitiated species with chain reactions that generate combustion radicals. However, detailed chemical kinetic models for hydrocarbon fuels are typically validated against experimental data obtained with clean or unvitiated air. Therefore, the need to develop accurate detailed kinetic mechanisms that account for varying thermophysical and chemical kinetic phenomena unique to vitiation has become an important aspect of combustion research.

In regard to combustion, vitiated air typically refers to an oxidizer stream with oxygen level less than that of normal air (i.e. $X_{O2} < 21$ vol %) and/or containing other products of combustion including CO_2, H_2O, CO and NO_X. Vitiated conditions are often the result of flue or exhaust gas recirculation (EGR) into a fresh air stream which also results in elevated temperatures, or due to staged combustion systems e.g. with additional fuel injected downstream of the primary burning zone. Vitiation can be found in many practical combustion systems including gas turbine combustors, automobile engines, and furnaces to reduce emissions and/or improve efficiency [**1**]. Vitiated combustion is also used in aircraft engines where fuel is injected into the turbine exhaust at low pressures to increase engine thrust [**2**].

Useful combustion characteristics for validation of kinetic mechanisms against experimental data are ignition, extinction, speciation, and flame structure. Representative data for each of these phenomena are often measured through ignition delay time, blow-out or laminar flame extinction, species profiles from chemical reactors and laminar flames, and laminar flame speed respectively. There is limited experimental data available in the literature for kinetic model validation regarding vitiated combustion of liquid fuels including aviation fuels. Much of the previous work has focused on the kinetic aspects of vitiation chemistry through oxidization [**3**,**4**,**5**] and ignition [**6**,**7**,**8**] in flow reactors. Fuller et al. [**6**,**7**,**8**] investigated the effect of vitiated air on the ignition characteristics of JP-8 in flow reactor experiments in which NO exhibited the highest impact among the vitiated species in promoting the ignition process.

The primary characteristic of vitiation is the role of the diluents, both through the overall reduction in O_2 concentration and the composition of the diluent itself. For most combustion devices, the diluents consist of CO_2, H_2O, CO, and NO_X. Concentrations of CO_2 and H_2O in a vitiated oxidizer stream can measure up to 10 vol %, while CO and NO_X concentrations are on the order of 0.2 vol % and 1000 ppmv respectively [**2**]. Studies utilizing ignition delay time measurements by Fuller et al. [**6**,**7**,**8**] found that overall dilution and NO_X had the most significant effect on ignition. However, unlike the ignition process, vitiated species influence pre- and post-flame zone chemistry, which plays a role on flame propagation phenomenon. . Therefore, the current study is focused on the effect of the most prevalent products of combustion found in the vitiated oxidizer: CO_2 and H_2O. Not only do CO_2 and H_2O comprise the majority of the non-N_2 diluent species in vitiated air, these components can also have significant thermophysical, transport and kinetic effects on the combustion process. The thermophysical property changes will have a direct effect on flame speed as they affect the flame temperature and thermal diffusion from the flame front to the unburned fuel. This combined with the chemical kinetic effects, which are less understood, results in significant changes in laminar flame speed when vitiated species are present in combustion air.

The primary objective of the current effort is to acquire laminar flame speed of aviation fuels with vitiated air that can be used to validate detailed kinetic models. In order to investigate the effect of vitiated species such as CO_2, H_2O and N_2 on laminar flame speed, *n*-decane is chosen as the fuel as it is often used as one of the surrogate components to model oxidation chemistry of *n*-alkanes in aviation fuels. For example, Gokulakrishnan et al. [**9**,**10**] used *n*-decane, iso-octane, *n*-propyl-cyclohexane and *n*-propyl-benzene as the surrogate components to model the combustion chemistry of *n*-alkanes, iso-alkane, cyclo-alkanes and aromatics respectively that are present in traditional petroleum based jet fuels. *n*-Decane is also used as one of the surrogate components to model the alternative jet fuels such as synthetic paraffinic fuels (e.g.,HRJ and S-8) [**11**]. *n*-Alkanes are generally more reactive during oxidation among the chemical groups mentioned above, hence they act as the main driver for the overall combustion characteristics of the jet fuels. Therefore, it is important to validate the chemical kinetic model for *n*-decane against experimental data obtained with vitiated air for accurate model predictions of JP-8 model under similar vitiated conditions. The current detailed kinetic model for *n*-decane, which is used in the surrogate kinetic model for JP-8, has been validated against species profiles obtained in reactivity [**12**,**13**] and time-history[**14**]

experiments in flow reactors as well as burned-stabilized laminar flame experiments [**15**]. An updated version of the detailed *n*-decane kinetic mechanism of Gokulakrishnan et al. [**9**,**10**,**11**] is used for the model comparison with the experimental data obtained in the current work.

Decane laminar flame speed measurements have been made by several groups using a variety of techniques. Nishiie et al. [**16**] measured laminar burning velocity and Markstein length of premixed *n*-decane flames at 1 atm and 400 K inlet temperatures using a spherical combustion chamber. Zhao et al. [**17**] measured the laminar flame speed of atmospheric pressure *n*-decane flames over a range of equivalence ratios. Flame speed was determined in a stagnation jet-wall configuration. The effect of nitrogen dilution was also investigated in this study. Ji et al. [**18**] measured laminar flame speeds of premixed C_5–C_{12} *n*-alkane flames, including decane, at atmospheric pressure and elevated unburned mixture temperatures. A counter-flow flame system was employed for these measurements. Kumar and Sung [**19**] measured laminar flame speed in a twin-flame counterflow configuration for atmospheric pressure flames at a range of preheat temperatures. A linear extrapolation method was used to obtain the laminar flame speed from the experimental methods.

At this time, little work has been done to characterize the effects of CO_2 and H_2O dilution on flame speed, especially in an effort to understand the chemical kinetics as they relate to other aspects of vitiation including variation in overall dilution, equivalence ratio and pressure. Zhao et al. [**20**] investigated the effect that overall dilution with N_2 has on propane flame speed. Those results show that dilution ratios up to 50% cause an approximate linear decline in flame speed for C_3H_8/air mixtures at temperatures of 300 K to 550 K and equivalence ratios of 0.8 to 1.1. Natarajan et al. [**21**] examined the effect of CO_2 dilution on multiple H_2/CO syngas mixtures at temperatures of 300 K to 600 K and pressures of 1 atm and 5 atm. Results of that study show the significant effect that 20% dilution of CO_2 has on flame speed of these syngas mixtures across a range of temperatures and pressures relevant to many vitiated combustion devices.

Because of the limited amount of study of flame speed with vitiation, especially for liquid fuels considered jet fuel surrogates, this study aims to better understand the effects of vitiation on the flame speed of *n*-decane through a two-pronged experimental program using the spherical Combustion Bomb Technique (CBT) (performed at Princeton University) with *n*-decane and the Bunsen Flame Technique (BFT) (performed at the Georgia Institute of Technology) with propane and *n*-decane. This approach provides a broader range of measurements as well as a cross-comparison at select conditions to allow a better understanding of differences between measurement techniques.

Experimental Methods

In order to examine the various effects of vitiation on laminar flame speed across a range of oxidizer compositions, temperatures and pressures, two separate measurement methods for measuring laminar flame speed are being applied in this study. The first, the spherical Combustion Bomb Technique (CBT), is being used to primarily examine the effects of vitiation on flame speed across a range of pressures relevant to both sub and super atmospheric combustion devices. The second method, applies the Bunsen Flame Technique (BFT) to measure laminar flame speed at fixed pressure and temperature, but at a range of equivalence ratios. Eventually, this technique will primarily focus on the effects of vitiation at atmospheric pressure and across a range of inlet temperatures. In order to understand not only the effects of vitiation, but also the range of measurement results between these techniques approximately 25% of the prescribed test cases in this study will be performed using both techniques to provide overlap comparison. A brief description of each technique is provided in the following sections.

Combustion Bomb Technique

In this study, the laminar flame speeds of *n*-decane in vitiated oxidizers consisting of various mixtures of O_2, N_2, CO_2, and H_2O was measured using the spherically outward propagating flame technique, or Combustion Bomb Technique,. Unlike counterflow and Bunsen flames, the spherical flame geometry provides the simplest and best defined flame geometries and boundary conditions for kinetic validation. By assuming quiescent burned gas and small flame curvature, the flame speed can be determined simply from the flame front trajectory and the density ratio. However, both flow compression in the confined vessel and flame stretch will affect the accuracy of the determination of flame speeds.

In this study, the flow compression and stretch corrected laminar flame speeds was be measured in a pressure range from 0.2 atm to 5 atm. These measurements serve to extend the LFS measurements made using the Bunsen Flame Technique to lower pressures and will provide measurements, made using a different technique, as

comparison. Vitiated conditions were be simulated by the addition of CO_2 and H_2O to the oxidizer consisting of O_2 and N_2/He.

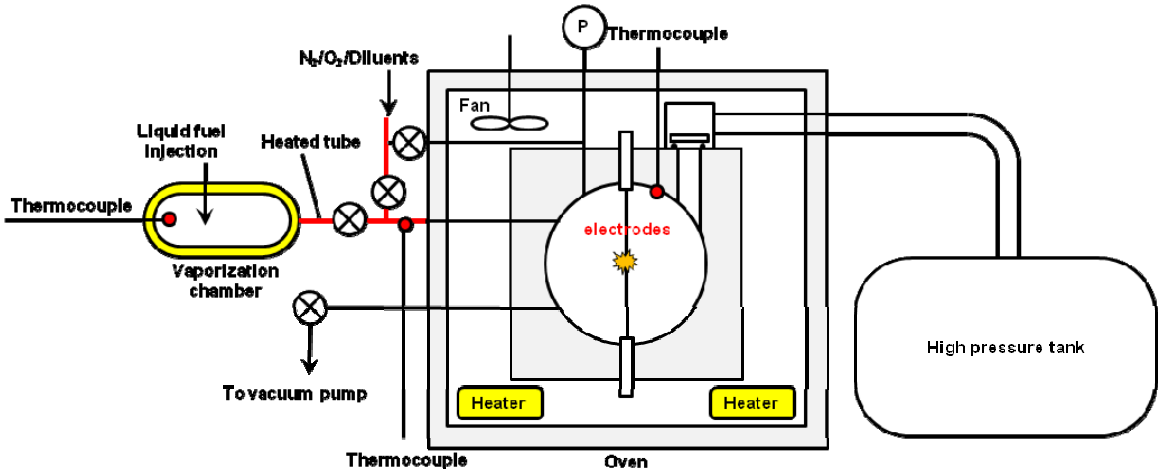

Figure 1: Schematic of the Combustion Bomb Technique (CBT) experimental facility.

The experimental setup is composed of a spherical combustion bomb, oven, pressure release system, and schlieren imaging system as shown in Figure 1. The spherical bomb has a 20 cm inner diameter. Two tungsten electrodes are installed in the top and bottom of the bomb and the upper electrode is mounted with a linear motion device to control the gap between the electrodes. The bomb is located inside of the oven, in which an electric fan is installed to achieve a uniform temperature field. Thermocouples at the top and bottom of the oven typically show a non-uniformity of 5 K. A K-type thermocouple is installed at upper right side of bomb to control the oven heater with a PID controller. The heated inlet lines and vaporization chamber are heated to the same temperature as the oven using separate PID controllers, K-type thermocouples, and resistance heaters.

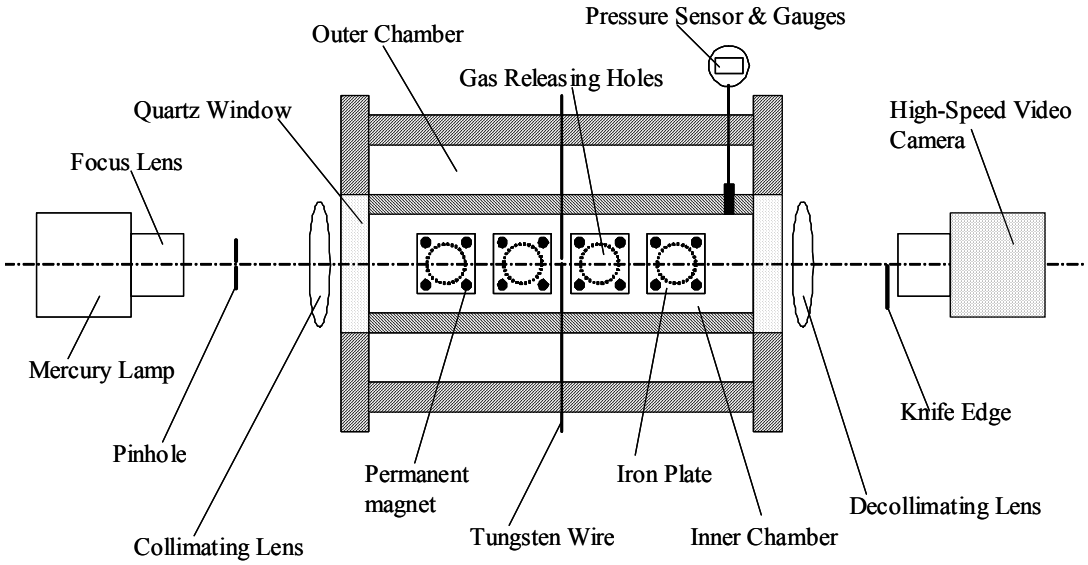

Figure 2: A schematic of the present pressure-release type high pressure combustion chamber and the high speed Schlieren imaging system.

Further detail of the spherically outward propagating flame experimental apparatus is shown in Figure 2. It is comprised of a dual combustion chamber and a high speed Schlieren imaging system. On the wall of the inner vessel, twelve holes (22 mm in diameter) with magnetically controlled doors allow for nearly constant pressure conditions during flame propagation. The apparatus has been tested to an operating pressure of 30 atm. Two quartz windows are mounted at both ends of the inner chamber to allow optical access. A high-speed Schlieren

photography system (8000 fps) is used in imaging the flame propagation (Figure 2). The unstretched flame speeds are extrapolated from the flame trajectory for flame diameters between 1.0 and 3.0 cm and pressure history by considering the flow and stretch corrections.

The bomb is filled with a combustible mixture using the partial pressure method. After vacuming to 2-3 torr, the bomb is filled with the bulk diluent (N_2 or He) to about 30 torr. This is done to fill the tubing leading to the pressure guage, which is at a lower temperature, so that fuel does not diffuse to this cooler location and condense. *n*-Decane (99% purity) is injected into the vaporization chamber (500 cc inner volume) and the vapor flows through a valve to the bomb. If water vapor is required, a separate vaporization chamber is used. The bomb is then filled with more diluents through the coiled 1/8" pressure tubing to push any fuel into the bomb, preventing condensation and removing rich pockets. Next, O_2 and other diluents are added through heated tubing. The gases that were used and their purities are: He (99.995%), O_2 (99.5%), CO_2 (99.99%), and N_2 (99.9%). The mixture is allowed 10 minutes to achieve uniformity, and then the mixture is ignited. The flame is visualized using a schlieren system with a mercury lamp and high speed camera (up to 15000 fps). Experimental uncertainty is finally determined from multiple tests at same equivalence ratio and pressure conditions.

Data analysis is performed in a manner similar to that previously reported by Burke et al. [**22**]. The flame front history is extracted from the schlieren images using an automated edge finding program. The burned flame speed and stretch rate [**23**] are then calculated. The burned unstretched flame speed is determined by extrapolating the flame speed to zero stretch using the linear stretch relation [**24**], and the unburned unstretched flame speed is found using the density ratio. Unlike [**22**], no flow correction is used in data analysis because the current study uses a large spherical chamber. According to Chen et al. [**25**], there is a 5% error due to compression induced flow when $R_f/R_{bomb} = 0.4$. In this study, data are used for $R_f/R_{bomb}<0.25$, so compression effects are neglected.

In order to prevent damage caused by excessive pressure build-up after ignition, a pressure release system is connected to the bomb. In this system, a 56.8 L nitrogen tank is connected to the bomb using two 1-1/2" pipes. Magnets, along with pressure from the nitrogen tank, push two plates onto two o-rings to seal two 1-1/2" holes in the bomb. After ignition, when the bomb pressure exceeds the nitrogen pressure, the seal between the plates and o-rings is broken, and gas from the bomb flows into the nitrogen tank, where the flame is quenched. The volume of the nitrogen tank is more than ten times the volume of the bomb, so the pressure of the system does not rise beyond acceptable levels.

Bunsen Flame Technique

Figure 3 is a schematic of the steady flow facility used to measure flame speeds using a Bunsen Flame Technique. The facility produces an axisymmetric jet flame over a contoured laminar nozzle. The reactant gas flows are metered individually with a bank of rotameters and introduced sufficiently far upstream to mix thoroughly before passing through the nozzle. Separate systems are used to vaporize the liquid water and fuel. The desired mixture of O_2, N_2 and CO_2 is used as a carrier gas for the water vaporizer. The output of the first vaporizer is then sent through the fuel vaporizer. The water flow rate is monitored by a mass flow controller, while the fuel flow rate is measured with a rotameter. The gas rotameters are calibrated at the same operating supply pressure with a wet test meter for high flow rates and a bubble flow meter for low flow rates. The liquid fuel rotameter is calibrated by operating the system for a fixed time and measuring the collected mass with a precision scale. The factory calibration is used for the water mass flow controller. The combined uncertainty (accuracy) in total mass flow rate is better than 1%.

The reactant mixture leaving the vaporizers is maintained at 420–470 K by electrically heated and insulated tubing until it reaches the burner plenum, where it is preheated to the desired temperature with electric resistance heaters. The temperature of the reactants is monitored with a K-type thermocouple placed 25 mm upstream of the exit. The flow entering the plenum passes through a layer of ball bearings that break up the incoming jet. A ceramic flow straightener (2 mm cell size) downstream removes any large scale structures before the flow enters the converging nozzle. The exit diameter of the contoured burner is 9 mm with an area-based contraction ratio of 72. This ensures that the exit velocity profile is uniform and the flow is laminar even at high Reynolds (Re) number. To anchor the flame at high flow rates (i.e., at high jet exit velocity to flame speed ratios), a sintered plate surrounding the nozzle exit is used to produce a near-stoichiometric, flat, methane–air pilot flame. The complete burner assembly is placed in a nitrogen ventilated chamber.

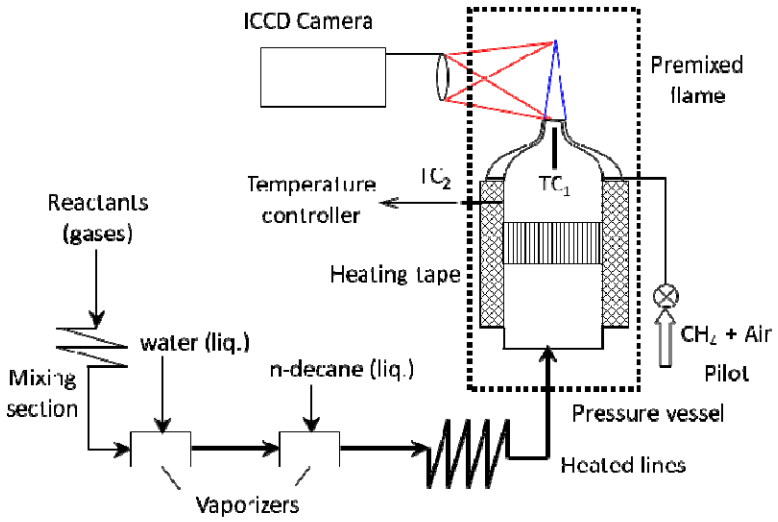

Figure 3: Schematic of the Bunsen Flame Technique (BFT) experimental facility.

Optical access for flame imaging is provided by three 5 cm diameter quartz windows. Broadband chemiluminescence images of the Bunsen flame are collected by an f/4.5, 105 mm UV Nikkor lens and recorded on a 16-bit ICCD camera. The camera is sensitive in the visible and ultraviolet range and capable of capturing CH*, OH* and CO_2* chemiluminescence from the flame. The magnification of the imaging system ranged from ~30–50 μm/pixel. Typical flame images are shown in Figure 4 for preheated *n*-decane flames with different oxidizer diluents. The image exposure times are a few milliseconds, and reveal the flames to be essentially axisymmetric and stable.

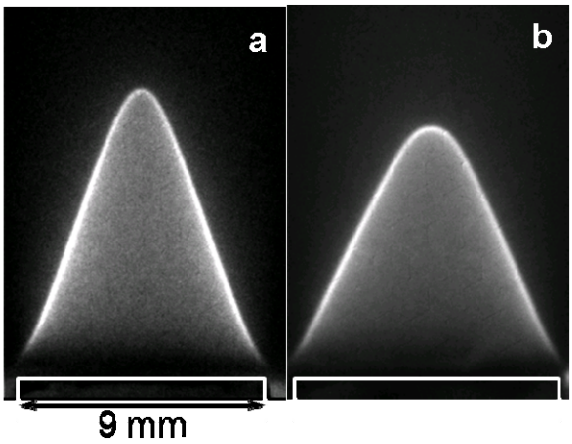

Figure 4: Instantaneous image of *n*-decane flame at 450 K, 1 atm, $\Phi \approx 1.0$. (a) O_2/N_2 = 18/82, (b) O_2/He/H_2O = 18/62/20.

An important difference between the current measurement approach and older Bunsen burner techniques is the definition of the appropriate flame area in this non-one dimensional flame and its reduction to flame speed. The method employed here depends on measuring the flame area at the reaction zone. The chemiluminescence images are analyzed to determine the reaction zone location with a gradient-based edge detection algorithm. The algorithm finds the inner edge of the reaction zone for both the left and right half images, from which the reaction zone area is calculated. The reaction zone areas from 50 realizations are then averaged to determine the flame area (A_b) at each operating condition. The unstretched, unburned flame speed (S_L) is then calculated from , where is the measured volumetric flow rate of the reactants. This procedure, which involves determining the reaction zone area as opposed to the inner edge of the preheat zone has been shown to provide a better estimate of the unstretched (1-d) flame speed, as it is only weakly affected by the flame curvature and because the Bunsen flame strain is primarily restricted to the low area flame tip [**21**].

Experimental Design

The goal of this effort is to better understand the effect of vitiation on the chemical kinetics of liquid fuel combustion. Therefore several variables found in many vitiated combustion systems were chosen as design variables for this study. The design variables include O_2 concentration, equivalence ratio, pressure, temperature and diluent composition. For most tests, the bulk diluent was N_2; however, for certain tests at varying pressures, the N_2 was replaced with He for comparative study and to inhibit high pressure flame stabilities that disrupt them measurements. The results presented here will focus on the role of total dilution, equivalence ratio, and pressure on laminar flame speed in relation to vitiated oxidizer composition.

Total dilution is determined by the variation of the concentration of O_2 in the oxidizer stream. Three O_2 levels were chosen: 21, 18, and 15 vol %. These volume fractions represent the amount of O_2 in the *oxidizer* stream only, not the overall inlet reactant stream including the fuel. This range of O_2 concentrations corresponds to the ranges used in a previous set of studies that examined the effect of vitiation on the ignition delay time of liquid fuel fuels [**6**,**7**]. For the second design variable, equivalence ratio (Φ), the values ranged from approximately 0.8 to 1.2. Pressure is examined at three levels: 0.5, 1.0, and 5.0 atm. This range covers both low-pressure combustion devices (e.g. high altitude propulsion systems, duct burners, etc.) as well higher pressure conditions often found many ground transportation and power generation systems.

The diluent composition variable consists of four different oxidizers compositions for a given O_2 concentration. The first set of cases consists of the "non-vitiated" cases in which the oxidizer consists of only O_2 and the bulk diluent (N_2 or He). For the three vitiated cases, 20 vol % of the bulk diluent (N_2 or He) in the oxidizer stream is replaced entirely with CO_2 or H_2O or a 10% CO_2 / 10% H_2O mixture. For example, a "non-vitiated" case with 18% O_2 would have the following oxidizer composition: 18% O_2 / 82% N_2 whereas a corresponding vitiated case could have the molar composition: 18% O_2 / 62% N_2 / 20% CO_2. The same format holds true for cases with 15 and 21 vol % O_2, cases with H_2O and CO_2/H_2O inclusion in the oxidizer stream, and whether the bulk diluent is N_2 or He. In the results discussed below, diluent mixtures will be denoted using the reference format shown in Table I. Table I also includes a comparison of thermodynamic data for cases with N_2 as the bulk diluent at 1 atm and 450 K at varying O_2 concentrations. Supplied specific heat and thermal diffusivity properties are given for the oxidizer stream alone. For each diluent composition, the value for the mixture of 18 vol% O_2 and N_2 as the bulk is given for molar heat capacity and thermal diffusivity due to small variation for each (±0.12% and ±0.01% respectively) in the range of 15 to 21 vol % O_2. With the higher molar specific heat, CO_2 produces a greater drop in adiabatic flame temperature compared to dilution with N_2 or H_2O.

Table I: Diluent Compositions and Thermodynamic Properties

	Vitiation Diluents		**Bulk Diluent Mole Fraction & T_{Ad} @ Φ = 1.0, 450 K, 1 atm X_{O2}:15 vol %, 18 vol %, 21 vol %**		**Ideal Gas Thermodynamic Property Comparison for Oxidizer Stream with 18% O_2 and N_2 as Bulk Diluent T = 450 K, P = 1 atm**	
Oxidizer Mixture	X_{CO2}	X_{H2O}	X_{Bulk}	T_{Ad} [K]	C_P [J/mol-K]	α [m^2/s]
O_2/N_2	0	0	0.85, 0.82, 0.79	1949, 2151, 2307	29.3	2.90E-05
$O_2/N_2/CO_2$	0.2	0	0.85, 0.82, 0.80	1809, 2003, 2157	31.3	2.60E-05
$O_2/N_2/H_2O$	0	0.2	0.85, 0.82, 0.81	1881, 2078, 2233	30.3	2.80E-05
$O_2/N_2/CO_2/H_2O$	0.1	0.1	0.85, 0.82, 0.82	1844, 2038, 2193	30.8	2.70E-05

A test matrix was developed to examine the role of diluent composition, total dilution, equivalence ratio and pressure on laminar flame speed of propane and *n*-decane. Multiple tests were conducted using both laminar flame speed measurement techniques, including a number of overlapping cases.

Results and Discussion

There are several effects of vitiation on the flame speed of *n*-decane that are observed in this study. The primary effect is caused by an increase in overall bulk dilution which in turn reduces the flame speed significantly due to the reduction in the flame temperature compared to fuel/air mixtures. Figure 5 shows the effect of N_2 dilution on laminar flame speed of stoichiometric *n*-decane/O_2/N_2 mixtures with varying dilutions at 450 K. In all the

experimental cases, the reduction of O_2 from 21 vol % to 15 vol %, signifying an increase in dilution, results in an approximate linear decrease in laminar flame speed. From a dilution standpoint, cases with 18 vol % O_2 signify volumetric dilution of air with an additional 16.7 % of N_2, while cases with 15 vol% O_2 signify a volumetric dilution of air with 40.0 % N_2. In Figure 5, most of the experimental data from the current study are from the BFT measurements. One point (at 18 vol% O_2) was acquired with the CBT and is in agreement with the BFT data (± 5%). Figure 5 also compares the current results to the propane experimental data of Zhao et al. [**20**] obtained with N_2 dilution at varying initial temperatures. Flame speed data at 450 K interpolated from Zhao et al.[**20**] and the current experimental data have a similar trend regarding the effect of N_2 dilution on laminar flame speed. Figure 5 also shows the detailed kinetic model predictions for the effect of N_2 dilution on *n*-decane flame speed. The *n*-decane laminar flame speed calculations were performed using Cantera [**26**] with the detailed kinetic mechanism of Gokulakrishnan et al. [**9**,**10**,**11**].

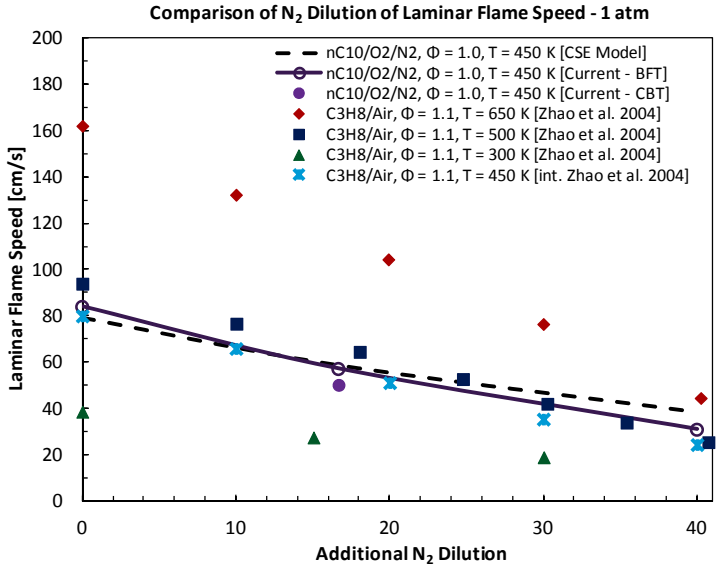

Figure 5: Comparison of N_2 dilution effect on laminar flame speed at 1 atm. C_3H_8 results are taken from Zhao et al. [**20**]. ***n*-Decane results are from the current study using the BFT (open circles) , CBT (closed circle), and CSE model predictions [9,10].**

Figure 6 shows the *n*-decane flame speed as a function O_2 concentration with varying bulk dilution composition as provided in Table I. Overall volumetric dilution was kept constant with 20% of the oxidizer stream varied between N_2, CO_2, H_2O and a 1:1 CO_2/H_2O mixture. For all tests, it was found that the presence of CO_2 in the diluents has the largest effect on flame speed. Replacement of 20 vol % of the oxidizer N_2 with CO_2 results in flame speeds that are lower by 40 to 60% of the corresponding measurements for O_2/N_2 cases. In the case of H_2O, a reduction in flame speed also occurred with measurements falling to values that are 60 to 90 % of the corresponding O_2/N_2 cases. As would be expected, mixtures with both H_2O and CO_2 result in flame speeds that fall between the CO_2 and H_2O only cases. Of greater interest is the interaction between diluent composition and the remaining design variables: total dilution, equivalence ratio, and pressure. Each of these interactions will be discussed in the following sub-sections.

Interaction of Diluent Composition and O_2 Concentration (Total Dilution)

The interaction examined between the effects of diluent composition and O_2 concentration (total dilution) is examined below. Flame speed data from measurements using both the CBT and the BFT for atmospheric tests performed with a preheat temperature of 450 K, N_2 as the bulk diluent, and an equivalence ratio of 1.0 are shown in Figure 6. The interaction between total dilution and dilution composition is shown in Figure 7, which compares the relative change in flame speed due to replacing 20 vol % of the oxidizer with CO_2, H_2O, or CO_2/H_2O at O_2 levels of 18 and 21 vol % O_2. When the oxidizer consists of 21 vol % O_2, replacing 20% N_2 with H_2O, CO_2/H_2O and CO_2 results in flame speeds that are markedly slower than normal air (89%, 67% and 45% of the flame speed with air respectively). When the total dilution is increased and O_2 makes up only 18 vol % of the oxidizer, the general effect

of dilution composition is more potent in reducing the flame speed. Replacing the same portion of the N_2 noted above with CO_2, CO_2/H_2O, and H_2O results in flame speeds that are 76%, 54% and 41% of the flame speed with 18% O_2/N_2 respectively. The results therefore show that changes in laminar flame speed due to diluent composition are enhanced as total dilution of the oxidizer stream increases and O_2 levels are reduced. This suggests that the effect of the dilution and dilution composition is not strictly a thermodynamic phenomenon, but has a significant chemical kinetic aspect as well.

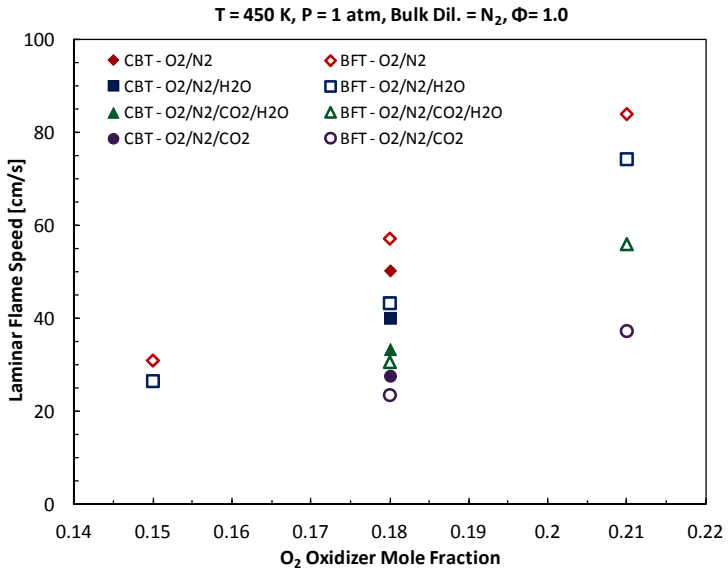

Figure 6: Experimental laminar flame speed measurements comparing total dilution (O_2 concentration) and diluent composition at 450 K, 1 atm and Φ = 1.0 with N_2 as the bulk diluent. Closed symbols: CBT; open symbols: BFT. CO_2, H_2O and CO_2/H_2O diluent compositions are noted above.

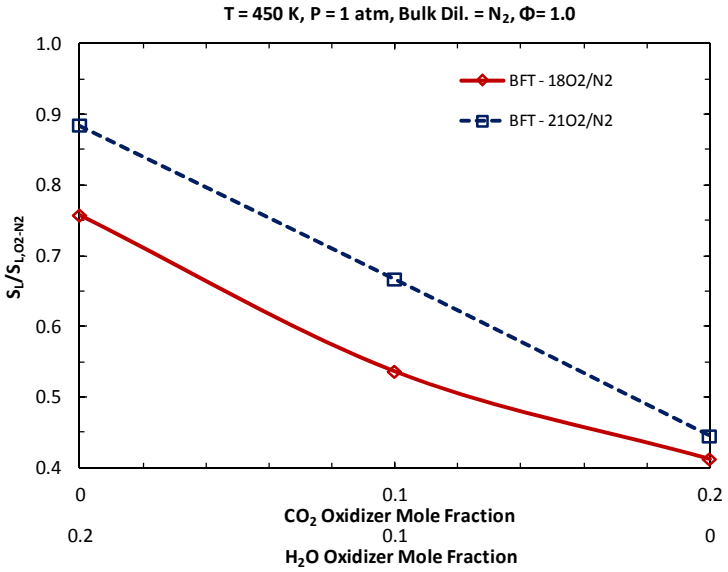

Figure 7: Relative laminar flame speed measurements comparing total dilution (O_2 concentration) and diluent composition at 450 K, 1 atm and Φ = 1.0 with N_2 as the bulk diluent. Relative measurements for a given O_2 concentration (e.g. X_{O2} = 0.18) are normalized to the corresponding measurement made for diluent compositions consisting only of O_2 and N_2 for the denoted O_2 concentration.

Interaction of Diluent Composition and Equivalence Ratio

The interaction between diluent composition and the equivalence ratio (Φ) of the system was also examined. Equivalence ratio was examined at lean (Φ = 0.8), stoichiometric (Φ = 1.0) and rich (Φ = 1.2) levels for the measurements made using the CBT. Measurements made using the BFT also covered a series of Φ's across this range. Experimental results with varying diluent composition from the measurements made by both techniques at 1 atm, preheat temperature of 450 K, and 18% O_2 in the oxidizer are shown in Figure 8. Overall, the flame speed measurements from both BFT and CBT have good agreement for the effect of diluents composition, except for the O_2/N_2 case. The BFT method shows slightly higher flame speeds compared to the CBT technique when the oxidizer stream consists of 18% O_2 in N_2. At all equivalence ratios CO_2 has the largest influence on flame speed compared to CO_2/H_2O and H_2O alone. Figure 8 also shows the detailed kinetic model predictions of Gokulakrishnan et al. [**9**,**10**]. Overall the model predicts the trends of the effect of dilution; however, model improvements are needed for more accurate predictions.

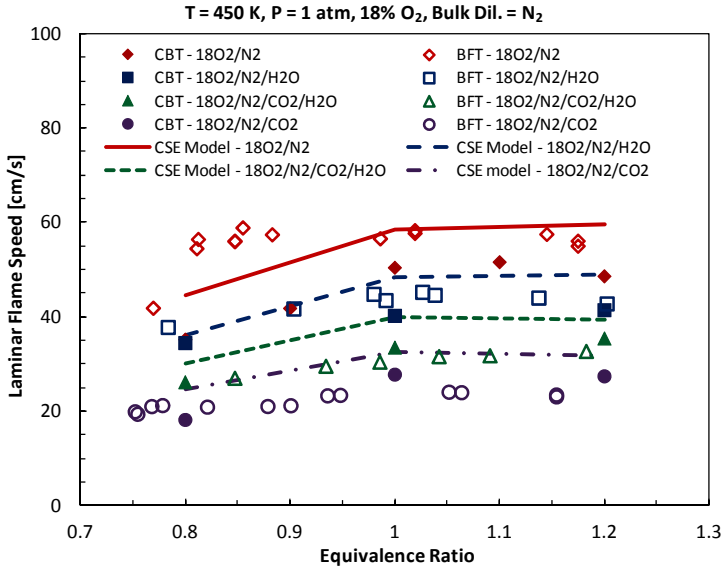

Figure 8: Experimental laminar flame speed measurements comparing equivalence ratio and diluent composition at 450 K and 1 atm with 18% O_2 and N_2 as the bulk diluent. Closed symbols: CBT; open symbols: BFT. CO_2, H_2O and CO_2/H_2O diluent compositions are noted above. Lines – model predictions [9,10] at Φ = 0.8, 1.0, & 1.2.

Figure 9 shows the laminar flame speed of *n*-decane mixtures with He as the bulk diluent using the CBT. A fraction of the oxidizer He is replaced in the oxidizer stream with CO_2, CO_2/H_2O and H_2O in the same proportions as shown for Table I for N_2. The presence of CO_2 and H_2O in with He has similar effects on flame speed as is found in the N_2 bulk dilution cases (shown in Figure 8). Figure 9 also shows the detailed model predictions of Gokulakrishnan et al. [**9**,**10**]. Overall, the model captures the absolute effect of CO_2 and H_2O diluents on flame speed somewhat better than in corresponding N_2 bulk dilution cases shown in Figure 8. This indicates that the lack of model agreement with the experimental data in Figure 8 for N_2 dilution is likely due in part to the uncertainties in the third body collision efficiencies used in the model for different diluent species.

An examination of the interaction between diluent composition and equivalence ratio is shown in Figure 10, which compares the relative change in flame speed due to substituting 20 vol % of the oxidizer stream with CO_2, H_2O, and CO_2/H_2O. Overall, the results in Figure 10 show that the equivalence ratio has less impact on the effect of the diluent composition on flame speed when He is the bulk diluent. For stoichiometric cases, replacing N_2 with H_2O, CO_2/H_2O and CO_2 results in flame speeds that are 80%, 66% and 55% of the stoichiometric flame speed with 18% O_2/N_2 respectively. For the rich case at Φ= 1.2, the effect of substituting N_2 with CO_2, CO_2/H_2O and H_2O has a slightly reduced effect on flame speed than the stoichiometric case. The largest difference is observed in the CO_2/H_2O case, where the relative flame speed from the 18% O_2/N_2, Φ = 1.2 case is only 73% compared to 66% for the analogous stoichiometric condition. The difference between the stoichiometric and rich cases with 20% CO_2 in the oxidizer is negligible. A crossover effect of the diluent composition with respect to equivalence ratio is seen in

the lean case of Φ = 0.8. The presence of 20% H_2O has nearly no effect on flame speed, while the presence of 20% CO_2 slightly reduces flame speed further for Φ = 0.8 than it does in either of the analogous stoichiometric and rich conditions.

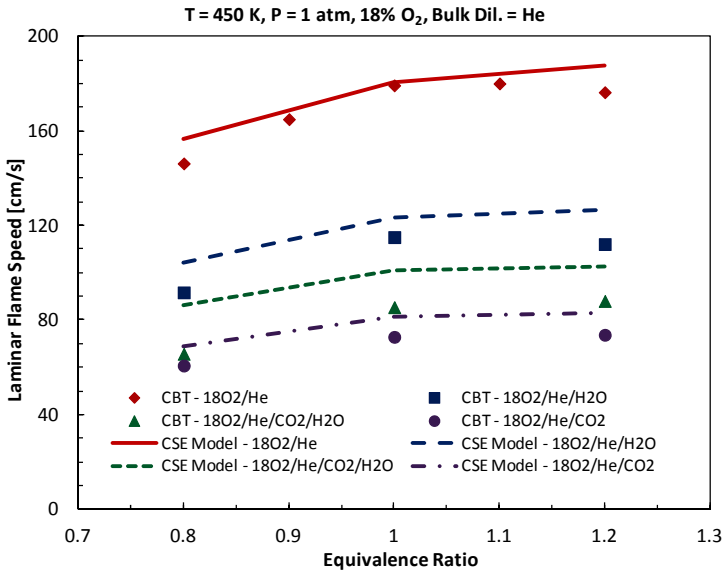

Figure 9: Experimental CBT laminar flame speed measurements comparing equivalence ratio and diluent composition at 450 K and 1 atm with 18% O_2 and He as the bulk diluent. Symbols: CBT; Lines – model predictions [9,10] at Φ = 0.8, 1.0, & 1.2.

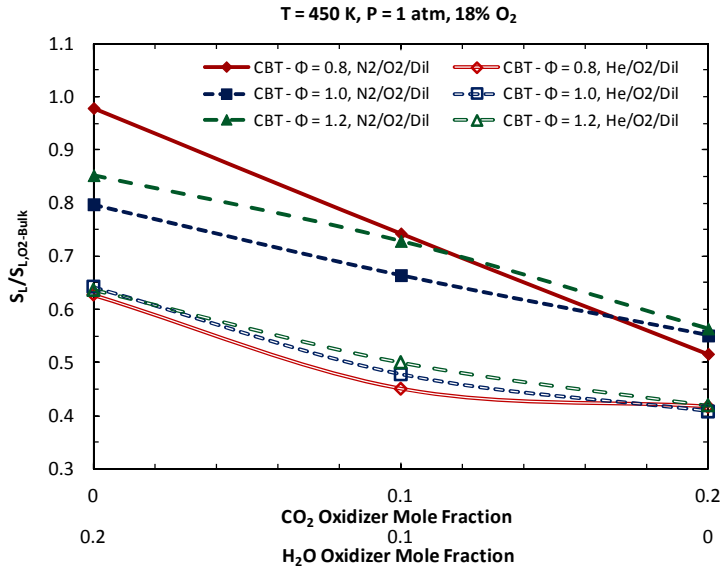

Figure 10: Relative laminar flame speed measurements using CBT comparing equivalence ratio and diluent composition at 450 K and 1 atm with 18% O_2 and both N_2 and He as the bulk diluent. Relative measurements for a given equivalence ratio (e.g. Φ = 0.8) are normalized to the corresponding measurement made for diluent compositions consisting only of 18% O_2 and N_2/He at the denoted Φ. Closed symbols: CBT O_2/N_2; open symbols: CBT O_2/He.

For the cases with He as the bulk diluent, there is very little variation in the effect of diluent composition with respect to equivalence ratio. For the cases with 20% CO_2 and 20% H_2O in the oxidizer stream, the effect is nearly

the same for all three equivalence ratios. There is some variation when 10% CO_2 / 10% H_2O is present in the oxidizer, however it is relatively small, ranging from 45% to 50%. The crossover effect from 20% H_2O to 20% CO_2 seen in the lean case ($\Phi = 0.8$) with N_2 as the bulk diluent is not observed with He.

Interaction of Diluent Composition and Pressure

The interaction between the composition of the diluent and the pressure of the system was also examined. In Figure 11, CBT flame speed measurements are shown at pressures of 0.5, 1.0 and 5.0 atm using He as the bulk diluent with varying the diluent compositions as noted in Table I. As expected, an increase in pressure reduces the flame speed and the substitution of the 20% of the oxidizer stream with CO_2 in place of He has the largest effect in reducing the flame speed compared to H_2O and CO_2/H_2O.

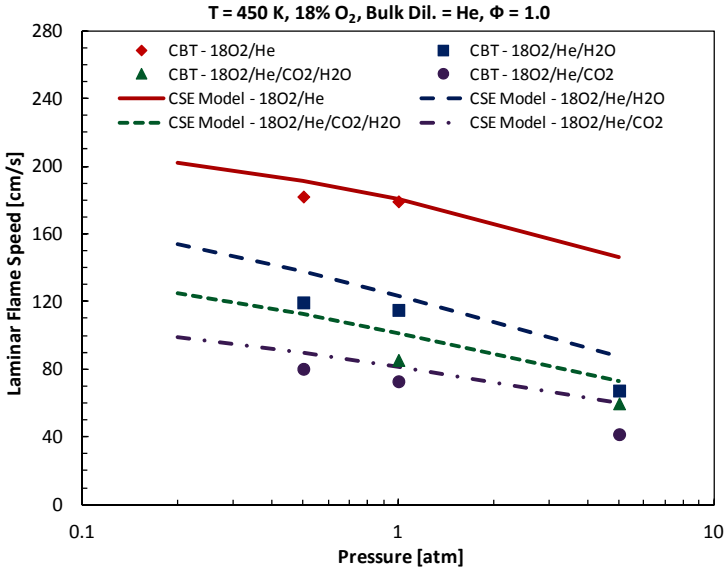

Figure 11: Experimental laminar flame speed measurements comparing pressure and diluent composition at 450 K and Φ = 1.0 with 18% O_2 and He as the bulk diluent. CO_2, H_2O and CO_2/H_2O diluent compositions are noted above.

In Figure 12, the relative change in CBT flame speed due to replacing a portion of the N_2 with CO_2, H_2O, or CO_2/H_2O is compared at pressures of 0.5 and 1.0 atm. The effect of CO_2 and H_2O varies by a very small margin between 0.5 and 1.0 atm. Unlike the interactions of diluent composition with total dilution and equivalence ratio, where the effect of the diluent composition varied significantly with changes in other variables, this data suggests that diluent composition has negligible impact on the effect of pressure on flame speed.

Kinetic vs. Thermal Effects

A focus of this study is to better understand the role that vitiation plays on combustion chemistry. As noted earlier and shown in Table I, there is a significant change in the thermodynamic properties of the system when a significant portion of the bulk diluent in the oxidizer stream is comprised of CO_2 or H_2O. This substitution impacts the flame speed primarily through a change in the flame temperature. To better isolate the kinetic effects from the thermodynamics of the system, simulations were performed using a detailed kinetic mechanism [**27**] that was validated for propane and compared against the experimental data obtained in the current work using the BFT. Figure 13 compares experimental laminar flame speed data for propane/air at 1 atm and a pre-heat temperature of 650 K as well as the same conditions with 10% added CO_2 dilution to the oxidizer stream. The model predictions for the undiluted cases as well as 10% dilution with N_2, H_2O and CO_2 are also shown.

In the case of CO_2 and H_2O, laminar flame speed calculations were performed in which the chemical kinetics of each of these diluents was disabled, designating these molecules as inert third bodies with thermodynamic and transport properties only. The figure shows that when CO_2 is made kinetically active; the model predictions agree with the experimental data very well. When CO_2 in oxidizer stream is made inert, the mechanism over predicts flame speed. This trend holds true for H_2O as well, where H_2O, as an active species, reduces the flame speed of

propane to a larger extent than by simply altering the thermodynamics of the system. However, when 10% N_2 is added to the oxidizer stream as inert species, the modeling results do not show any significant difference as noted in Figure 13. Based on the modeling results in Figure 13, the presence of CO_2 in the oxidizer shows not only the larger overall effect on flame speed, but the larger kinetic effect as well when compared to H_2O. This is similar to the experimental findings of this study with *n*-decane.

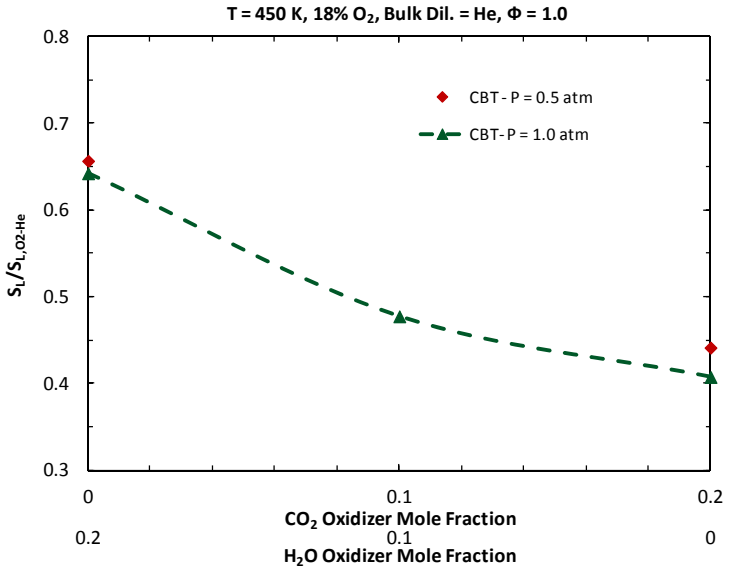

Figure 12: Relative laminar flame speed measurements comparing pressure and diluent composition at 450 K and Φ = 1.0 with 18% O_2 and He as the bulk diluent. Relative measurements for a given pressure (e.g. 1.0 atm) are normalized to the corresponding measurement made for diluent compositions consisting only of O_2 and He for the denoted pressure.

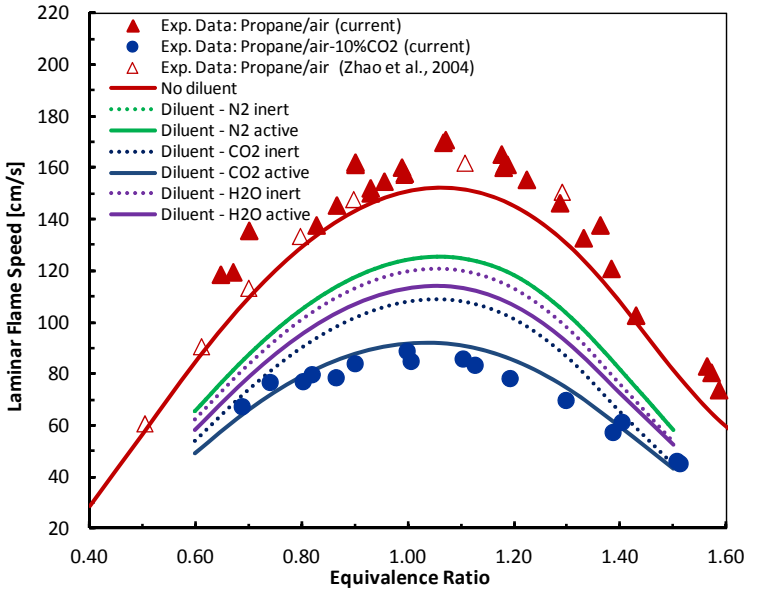

Figure 13: Comparison of thermal and kinetic effects of CO_2 dilution in a propane-air flame at 1 atm and 650 K against model predictions with CO_2 and H_2O as both chemically active and inert diluents. .

Figure 14 shows the normalized sensitivity coefficients for propane flame speed with 10% CO_2 addition as inert and active species for the cases discussed in Figure 13. As expected the most sensitive reaction is the branching reaction (R1)

$H + O_2 = OH + O$ (R1)

The second most sensitive reaction is that which produces CO_2 from CO:

$CO + OH = CO_2 + H$ (R2)

When CO_2 is introduced as a chemically active species, it reduces the H production via reaction (R2). This will in turn reduce the overall radical concentration from chain-branching reaction (R1). This results in a reduction in the flame speed when CO_2 is present in the vitiated air.

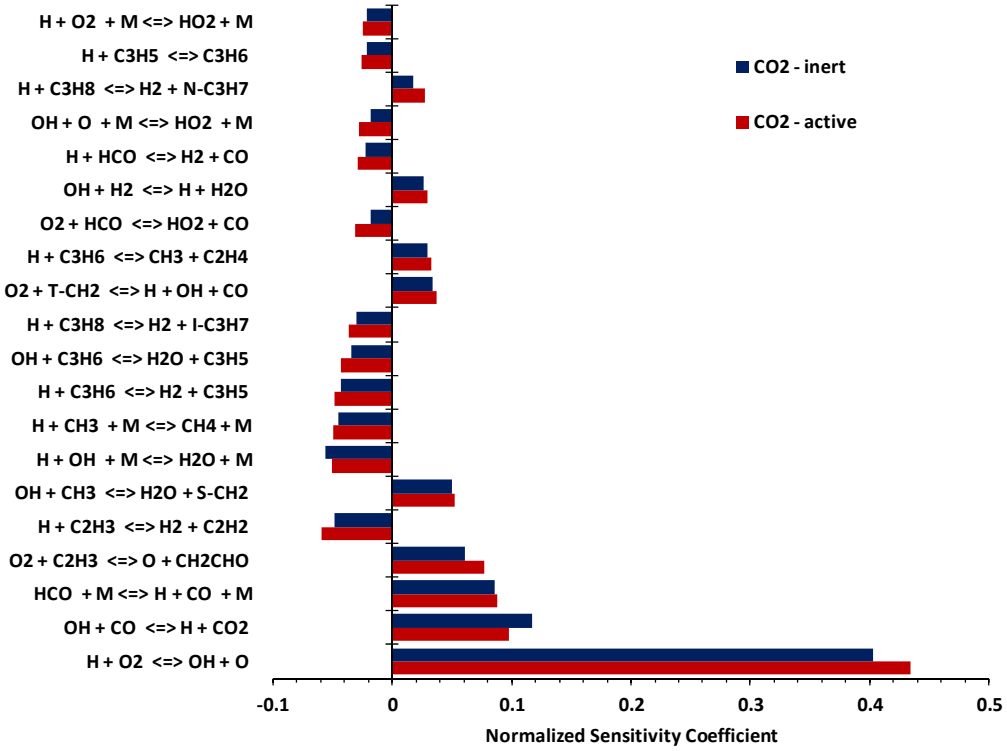

Figure 14: Normalized sensitivity coefficients for laminar flame speed of propane in air/10% CO_2 at 650 K and 1 atm

Conclusions

As combustion research extends further into the realm of vitiated kinetics, experimental and theoretical analyses continue to show that vitiation significantly alters the combustion processes and flame characteristics due to both thermodynamic changes to the system and chemical kinetic interactions. Through the examination of overall oxygen dilution and the presence of CO_2 and H_2O in the oxidizer stream, this study has found that the flame speed of propane and, more importantly to better understand aviation fuel combustion, *n*-decane is significantly affected by oxidizer vitiation. The reduction of O_2 alone from 21 vol % typical of normal air to 15 vol % found in many vitiated combustion devices is shown to reduce *n*-decane flame speeds on the order of 60%, whereas even larger reduction is seen when O_2 reduction is due to the presence of combustion products CO_2 and H_2O in the oxidizer. More importantly, the experimental data and kinetic analysis of the presence of CO_2 and H_2O in the oxidizer stream illustrate that the effects of vitiation are not merely thermodynamic but also the chemical kinetics of the oxidization processes in the presence of vitiated species. This observation is in contrast to the effect of CO_2 and H_2O on JP-8 ignition delay time studied in another related work by Fuller et al. [**6**,**7**,**8**], in which NO_X has the most significant effect in promoting the oxidation. These experimental data are useful additions to the literature for current and future model validation for vitiated kinetics. At this time, the current detailed model shown in this study offers good predictions for the effects of vitiation on *n*-decane flame speed; however, further development is required to improve accuracy.

Bibliography

[1] A. Cavaliere and M. de Joannon, "Mild Combustion," *Progress in Energy and Combustion Science*, vol. 30, pp. 329-366, 2004.

[2] J. A. Lovett, T. P. Brogan, S. P. Derk, B. V. Kiel, and T. V. Thompson, "Development Needs for Advanced Afterburner Designs," in *40th AIAA/ASME/SAE/ASEE Joint Propulsion Conference and Exhibit*, vol. AIAA 2004-4192, Fort Lauderdale, Florida, 2004.

[3] S. Kowalski, "A Study of the Low and Intermediate Temperature Oxidiation Chemistry of a Primary Reference Fuel Blend and Two Gasolines at High Pressure," Department of Mechanical and Aerospace Engineering, Princeton University, Masters Thesis 1993.

[4] G. Moreac, P. Dagaut, J. F. Roesler, and M. Cathonnet, "Nitric oxide interactions with hydrocarbon oxidation in jet-stirred reactor at 10 atm," *Combustion and Flame*, vol. 145, pp. 512-520, 2006.

[5] A. Dubreuil, F. Foucher, C. Mounáim-Rousselle, G. Dayma, and P. Dagaut, "HCCI combustion: Effect of NO in EGR," in *Proceedings of the Combustion Institute*, vol. 31, 2007, pp. 2879-2886.

[6] C. C. Fuller, P. Gokulakrishnan, M. S. Klassen, R. J. Roby, and B. V. Kiel, "Investigation of the Effects of Vitiated Conditions on the Autoignition of JP-8," *45th AIAA/ASME/SAE/ASEE Joint Propulsion Conference & Exhibit*, vol. AIAA 2009-4295, August 2009.

[7] C. C. Fuller, P. Gokulakrishnan, M. S. Klassen, R. J. Roby, and B. V. Kiel, "Investigation of the Effect of Nitric Oxide on the Autoignition of JP-8 at Low Pressure Vitiated Conditions," *Proceedings of the American Institute of Aeronautics and Astronautics*, 2011.

[8] C. C. Fuller, "Investigation of JP-8 Autoignition Under Vitiated Combustion Conditions," Mechanical Engineering, University of Maryland, College Park, MD, M.S. Thesis 2011.

[9] P. Gokulakrishnan, G. Gaines,, J. Currano, , M. S., Klassen, and R. J. Roby, "Experimental and Kinetic Modeling of Kerosene-Type Fuels at Gas Turbine Operating Conditions," *Journal of Engineering for Gas Turbines and Power*, vol. 129, pp. 655-663, 2007.

[10] P. Gokulakrishnan, G. Gaines, M. S. Klassen, and R.J. Roby, "Autoignition of Aviation Fuels: Experimental and Modeling Study," in *AIAA/ASME/SAE/ASEE 43rd Joint Propulsion Conference*, vol. AIAA 2007-5701., Cincinnati, OH, 2007.

[11] P. Gokulakrishnan, M. S. Klassen, and R. J. Roby, "Ignition Characteristics of A Fischer-Tropsch Synthetic Jet Fuel," in *ASME Turbo Expo 2008: Power for Land, Sea and Air*, Berlin, Germany, 2008, pp. GT2008-51211.

[12] P. Dagaut, M. Reuillon, J-C. Boettner, and M. Cathonnet, "“Kerosene Combustion at Pressures upto 40 atm: Experimental Study and Detailed Chemical Kinetic Modeling," *Proceeding of the Combustion Institute*, vol. 25, pp. 919-926, 1994.

[13] P. Dagaut, "On the Kinetics of Hydrocarbons Oxidation from Natural Gas to Kerosene and Diesel Fuel”," *Physical Chemistry and Chemical Physics*, vol. 4, pp. 2079 –2094, 2002.

[14] S. P. Zeppieri, S. D. Klotz, and F. L. Dryer, "Modeling Concepts for Large Carbon Number Alkanes: A Partially Reduced Skeletal Mechanism for n-Decane Oxidation and Pyrolysis," *Proceedings of the Combustion Institute*, vol. 28, pp. 1587–1595, 2000.

[15] C. Douté, J. L. Delfau, R. Akrich, and C. Vovelle, "Chemical Structure of Atmospheric Pressure Premixed n-Decane and Kerosene Flames," *Combustion Science and Technology*, vol. 106, pp. 327–344, 1995.

[16] T. Nishiie, D. Singh, and L. Qiao, "Laminar Burning Velocity and Markstein Length of n-Decane/Air, Jet-A/Air, and S-8/Air Flames," in *Proceedings of the 6th U.S. National Combustion Meeting*.

[17] Z. Zhao, J. Li, A. Kazakov, and F. L. Dryer, "Burning velocities and a high-temperature skeletal kinetic model for n-decane," *Combustion Science and Technology*, vol. 177, no. 1, pp. 89-106, 2005.

[18] C. Ji, E. Dames, Y. L. Wang, and F. N. Egolfopoulos, "Propagation and extrinction of premixed C5-C12 n-alkane flames," *Combustion and Flame*, vol. 157, no. 2, pp. 277-287, 2010.

[19] K. Kumar and C. J. Sung, "Laminar flame speeds and extinction limits of preheated n-decane/O2/N2 and n-dodecane/O2/N2 mixtures," *Combustion and Flame*, vol. 151, pp. 209-224, 2007.

[20] Z., Kazakov, A., Li, J. and Dryer, F. L. Zhao, "The Initial Temperature and N2 Dilution Effect on the Laminar Flame Speed of Propane/air," *Combustion Science and Technology*, vol. 176, pp. 1705-1723, 2004.

[21] J. Natarajan, T. Lieuwen, and J. Seitzman, "Laminar flame speeds of H2/CO mixtures: Effect of CO2 dilution, preheat temperature, and pressure," *Combustion and Flame*, vol. 151, pp. 104-109, 2007.

[22] M. P. Burke, M. Chaos, F. L. Dryer, and Y. Ju, "Negative pressure dependence of mass burning rates of H2/CO/O2/diluent flames at low flame temperatures," *Combustion and Flame*, vol. 157, no. 4, pp. 618-631, April 2010.

[23] R. A. Strehlow and L. D. Savage, "The concept of flame stretch (non strictly one dimensional premixed laminar flame propagation modes)," *Combustion and Flame*, vol. 31, no. 2, pp. 209-211, 1978.

[24] G. H. Markstein, *Nonsteady flame propagation*. New York, USA: Pergamon, 1964.

[25] Z. Chen, M. P. Burke, and Y. Ju, "Effects of compression and stretch on the determination of laminar flame speeds using propagating spherical flames," *Combustion Theory and Modelling* , vol. 13, no. 2, pp. 343-364, 2009.

[26] D. Goodwin. Cantera. [Online]. www.cantera.org

[27] "Chemical-Kinetic Mechanisms for Combustion Applications", San Diego Mechanism web page, Mechanical and Aerospace Engineering (Combustion Research), University of California at San Diego. [Online]. http://www.mae.ucsd.edu/~combustion/cermech/